A bio inspired learning scheme for the fractional order kidney function model with neural networks

Zulqurnain Sabir [a], Shahid Ahmad Bhat [b,*], Hafiz Abdul Wahab [c], Maria Emilia Camargo [d], Gulmira Abildinova [e], Zhandos Zulpykhar [e]

[a] Department of Computer Science and Mathematics, Lebanese American University, Beirut, Lebanon
[b] LUT Business School, LUT University, P.O. Box 20, FIN-53851 Lappeenranta, Finland
[c] Department of Mathematics and Statistics, Hazara University, Mansehra, Pakistan
[d] Graduate Program in Administration, Federal University of Santa Maria, Santa Maria 93458, Brazil
[e] L.N. Gumilyov Eurasian National University, Department of Computer Science, Astana, Kazakhstan

ARTICLE INFO

ABSTRACT

The numerical procedures of the fractional order kidney function model (FO-KFM) are presented in this study. These derivatives are implemented to get the precise and accurate solutions of FO-KFM. The nonlinear form of KFM is separated into human (infected, susceptible, recovered) and the components of water (calcium, magnesium). Three cases of FO-KFM are numerically accessible using the stochastic computing scaled conjugate gradient neural networks (SCJGNNs). The statics assortment is performed to solve the FO-KFM, which is used as 78 % for verification and 11 % for both endorsement and training. The precision of SCJGNNs is achieved using the achieved and source outcomes. The reference solutions have been obtained by using the Adam numerical scheme. The competence, rationality, constancy is observed through the SCJGNNs accompanied by the imitations of state transition, regression performances, correlation, and error histograms measures.

1. Introduction

Water is a need of the life, which is very important for the health to drink enough water for every living being. One of the forms of the water is hard water, which affects the health of individual and contains the higher substance concentrations (calcium, magnesium) [1]. The continuous use of hard water can create the kidney dysfunction, which creates numerous diseases, like diabetes and cerebrovascular [2]. The people of Nusa Tenggara Timur (NTT) consumed the water based on different foundations, which are operated for average tenacities along with the higher percentages of calcium and magnesium. NTT people suffer the kidney disease among four provinces with higher ratio [3]. Therefore, it is important to know that how affects the people's health by using the hard water. For the required productivity based on different indications, a detailed assessment is mandatory. Such evaluations and consequences with different statistics are available. To find the better performances, the reduction of illnesses or spread of infection is characteristically used to evaluate the issues of public health.

Mathematical modeling is used to solve various complicated systems, some of the applications of these models are the pattern/classification recognition [4], metadata base system for semantic image [5], transmission network expansion planning [6], potato inspection using machine vision [7], waterborne spread/disease control [8], and cell-mediated immune response to tumor growth [9].

This research shows the simulations of fractional order kidney function model (FO-KFM) by applying the stochastic scaled conjugate gradient neural networks (SCJGNNs). The stochastic applications have been exploited in various stiff and complicated models, e.g., fluid dynamics models [10], Liénard differential model [11] and food chain nonlinear model [12]. The minute specifics using the super slow and superfast transition are scrutinized, which shows more topographies by applying the fractional derivatives that is considered difficult for the integer order complements. Moreover, the model dynamics is done by applying the fractional calculus, which performs better in comparison to integer derivatives by using the accessibility of condition. These derivatives have been implemented to verify the system's performance of the real-world submissions. The fractional calculus is generally accomplished to the last 3 decades by applying the considerable operatives. The above-mentioned fractional operators have their individual significance and worth. Whereas the most extensively Caputo derivative (CD)
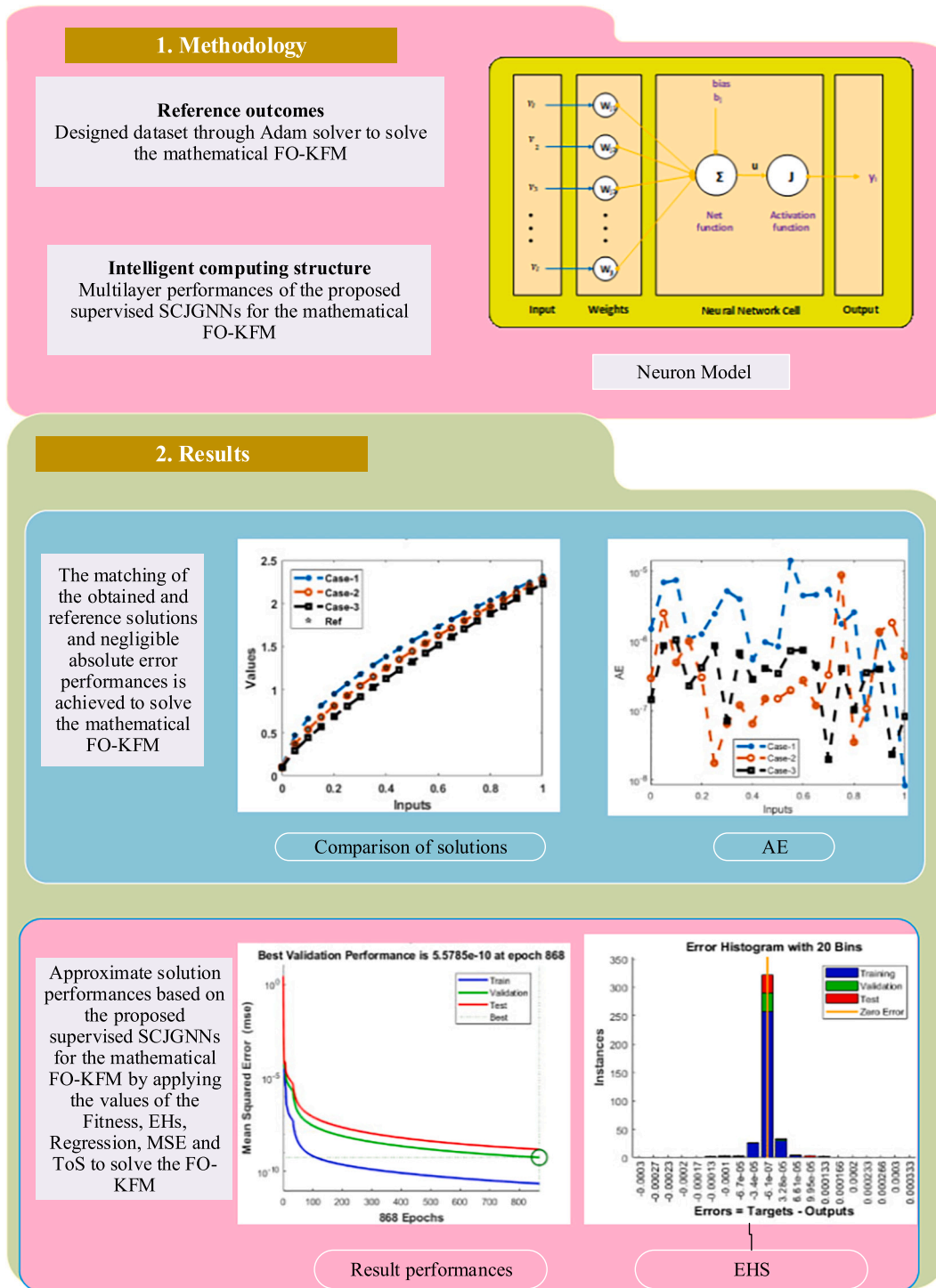
**Fig. 1.** Illustrations of SCJGNNs to solve the FO-KFM.

definition is used to present the solutions of homogeneous and non-homogeneous initial conditions and easy to execute. In view of all the FO applications and stochastic solvers, authors are inspired to present the solutions of the FO-KFM.

The other paper parts are shown as: FO-KFM is presented in Section 2. Designed structure of the SCJGNNs is shown in Section 3. Numerical performances are shown in Section 4. Conclusions are listed in Section 5.
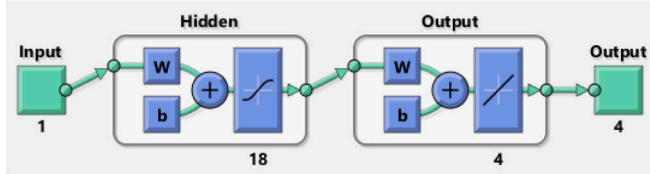
2. Mathematical FO-KFM

The mathematical structure based on the FO-KFM is presented in this section, which is divided into human (infected, susceptible, recovered) and the water components (calcium, magnesium). Three FO-KFM cases have been solved by operating the SCJGNNs, which is mathematically shown as [13]:
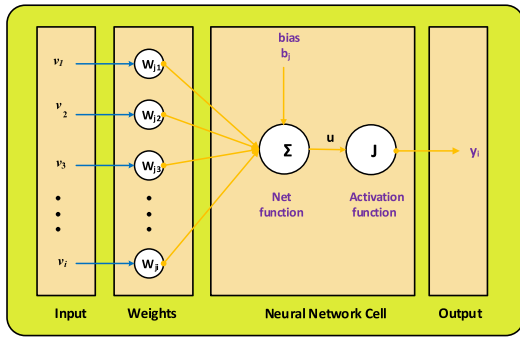
(a) Single neuron network structure

(b) Single, hidden and output layers using 18 neurons

Fig. 2. Single and multiple layers to solve the FO-KFM using the SCJGNNs, (a) Single neuron network structure, (b) Single, hidden and output layers using 18 neurons.

$$
\begin{cases}
\dfrac{dS(v)}{dv} = A - \beta\lambda(W)S(v) - \mu S(v), \\[2mm]
\dfrac{dI(v)}{dv} = \beta\lambda(W)S(v) - \gamma I(v) - \mu I(v), \\[2mm]
\dfrac{dR(v)}{dv} = \gamma I(v) - \mu R(v), \\[2mm]
\dfrac{dW(v)}{dv} = bW(v)\left(1 - \dfrac{W(v)}{K}\right) - cW(v).
\end{cases}
\tag{1}
$$

The human population using the susceptible birth is taken as a rate A. $\beta\lambda(W)$ shows the regular use of hard water, which is distressed to kidney dysfunction. The treating water procedure reasons a decrement rate at c using the compounds (magnesium, calcium). The recovered part is γ, b is the concentration of compound (calcium, magnesium) water, which is limited enhanced at rate K. β is the magnesium and calcium ratio of water, $\lambda(W)$ shows the ingestions prospect and the values of λ are taken between 0 and 1. Furthermore, the individual's ratio by using the kidney dysfunction based on the water's calcium/magnesium concentration, which is given as $\lambda(W) = \frac{W(v)}{W(v)+K}$. The fractional kind of the mathematical KFM is shown as:

$$
\begin{cases}
\dfrac{d^{\alpha}S(v)}{dv^{\alpha}} = A - \beta\lambda(W)S(v) - \mu S(v), \\[2mm]
\dfrac{d^{\alpha}I(v)}{dv^{\alpha}} = \beta\lambda(W)S(v) - (\gamma + \mu)I(v), \\[2mm]
\dfrac{d^{\alpha}R(v)}{dv^{\alpha}} = \gamma I(v) - \mu R(v), \\[2mm]
\dfrac{d^{\alpha}W(v)}{dv^{\alpha}} = bW(v)\left(1 - \dfrac{W(v)}{K}\right) - cW(v),
\end{cases}
\tag{2}
$$

where α represents the fractional CD to solve the FO-KFM, which is shown in above system (2). The FO derivative values are used in the interval 0 and 1. These derivatives are unified to perceive the minute particulars (super slow and superfast transients), which is tough to recognize through the integer order. Recently, FO derivatives are applied in many applications, like time-delayed genetic regulatory networks [14], tobacco smoking model containing snuffing class [15], and gene regulatory networks [16]. The novel topographies of this work are

Table 1
Implementation and parameter setting.

Parameter	Settings
Authorization and training	11 %
Testing	78 %
Decreeing Mu values	0.2
Maximum iteration	1000
Increasing Mu factor	12
Maximum mu performances	10^{08}
Reference dataset	Adam solver
Number of neurons	18
Fitness	0
Output/hidden and input layers	Single
Minimum gradient values	10^{-06}
Stoppage specifications	Default
Adaptive Mu values	0.0005
Selection of samples	Arbitrary

shown as:

- The design of the FO is accessible to perform the accurate numerical results of mathematical KFM.
- The present soft computing performance based on the designed structure is not executed before to solve FO-KFM.
- The precision of stochastic SCJGNNs is provided by using the outcomes comparisons.
- A reduceable absolute error (AE) represents the competency of proposed SCJGNNs to solve the FO-KFM.
- The error histograms (EHs), transition of state (ToS), and regression measures enhance the dependability of FO-KFM.

3. Proposed SCJGNNs method

This section presents the methodology of the proposed SCJGNNs to solve the mathematical FO-KFM. The methodology is performed using the essential execution of the practice together with some numerical computing phases. Fig. 1 shows the stepwise system depictions using the operative performances of the FO-KFM. The first phase shows the framework of the model, system expressions to solve the nonlinear dynamics of the FO-KFM are presented in second step, third phase shows the SCJGNNs presentations, while the last step presents the numerical results.

The dataset by performing the epochs based on the FO-KFM is provided to get the standard outputs, which are presented in Fig. 2(a) using the "NDSolve" in Mathematica. The comparison assessments also perform the generation of the data for FO-KFM. The performances of the SCJGNNs are implemented to get the wide-ranging observation of the system based single neurons is presented in Fig. 2(b). The procedure based SCJGNNs is provided using the 'nftool' command in 'Matlab' with appropriate hidden layers including testing, learning and corroboration statics. The implementing setting of the parameter using the proposed structure for the FO-KFM is presented in Table 1.

4. Numerical solutions

This section is based on three cases of the FO-KFM using the SCJGNNs, which is mathematically shown as:

Case 1 to 3 is presented by taking $\alpha = 0.6$, 0.7 and 0.8, while the other values $\mu = \frac{1}{65}$, $\gamma = \frac{1}{45}$, $\beta = \frac{1}{100}$, $K = 60$, $b = \frac{1}{10}$, $c = \frac{2}{5}$, $A = 2$, $S_0 = 0.1$, $I_0 = 0.2$, $W_0 = 0.3$ and $R_0 = 0.4$ are taken in Eq. (1). The obtained results have been obtained by applying the designed SCJGNNs procedure to solve the nonlinear FO-KFM. The input interval has been taken between 0 and 1 to solve the mathematical FO-KFM. Eighteen neurons with the selection of data have been used together with the selection of training, authentication, and testing. Fig. 3 shows the obtained results by applying the SCJGNNs for the nonlinear FO-KFM along with the best corroboration values and ToS. The best authentication performances are
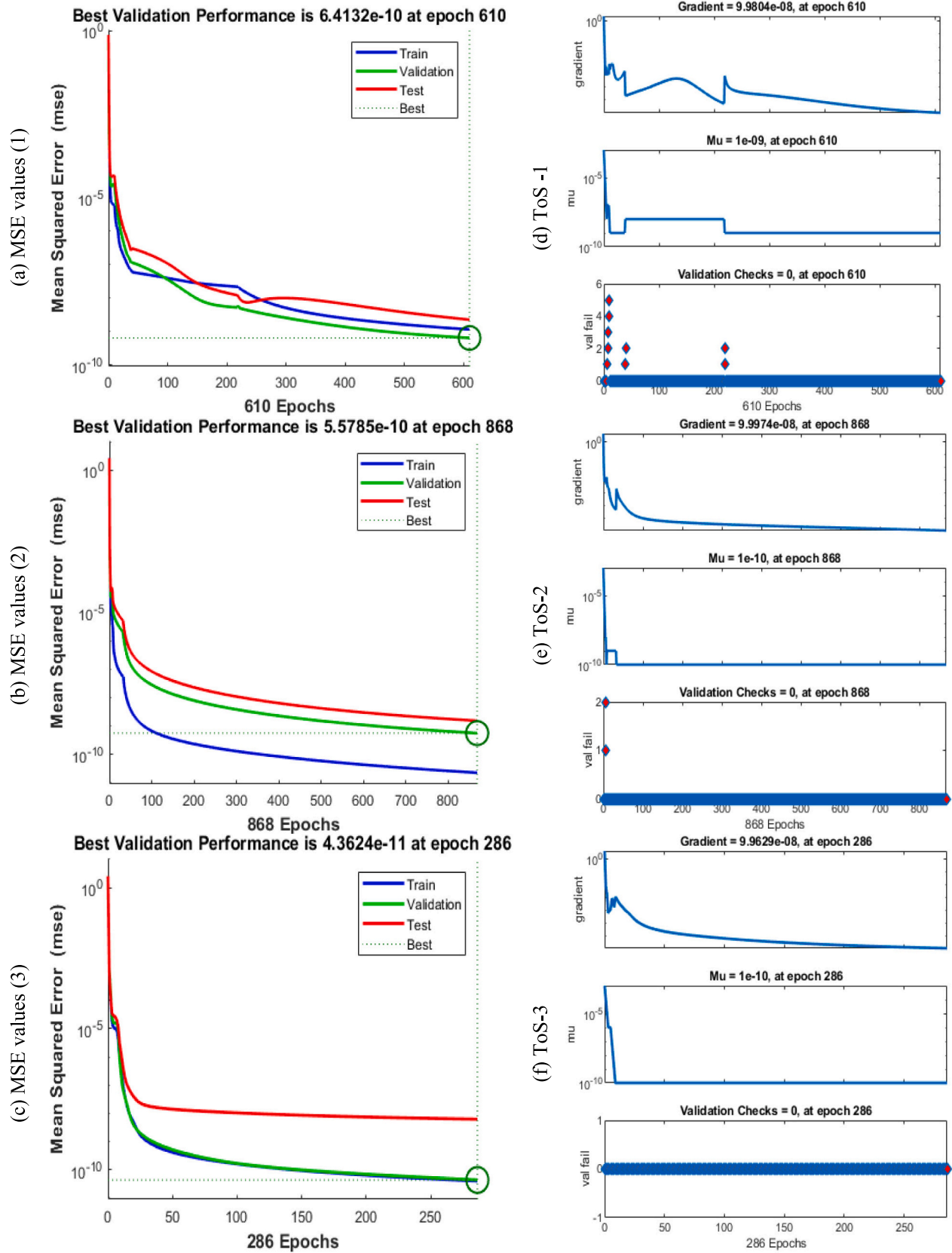
Fig. 3. Performances of MSE and ToS for the nonlinear FO-KFM, (a) MSE values (1), (b) MSE values (2), (c) MSE values (3), (d) ToS-1, (e) ToS-2, (f) ToS-3.

Z. Sabir et al.

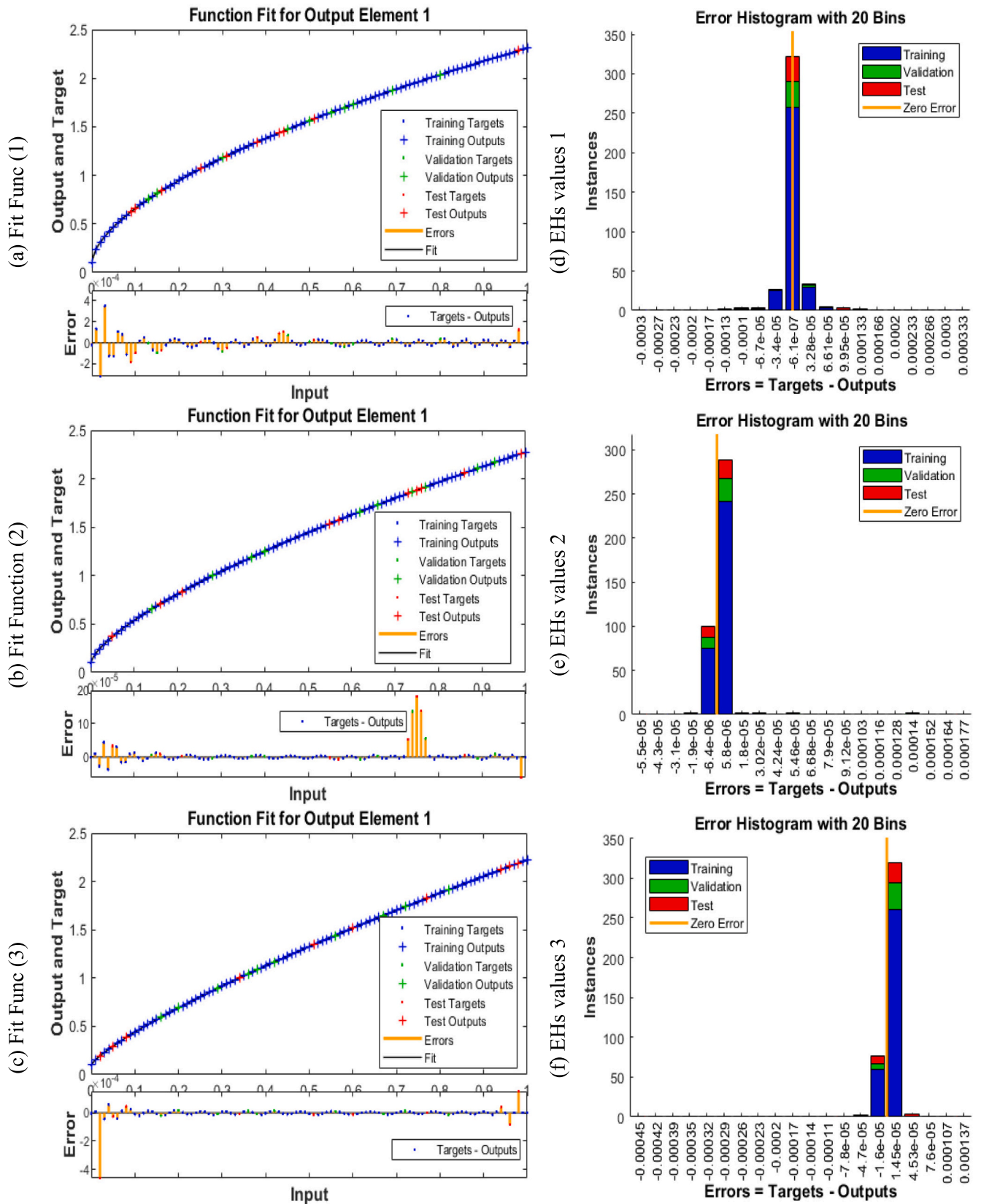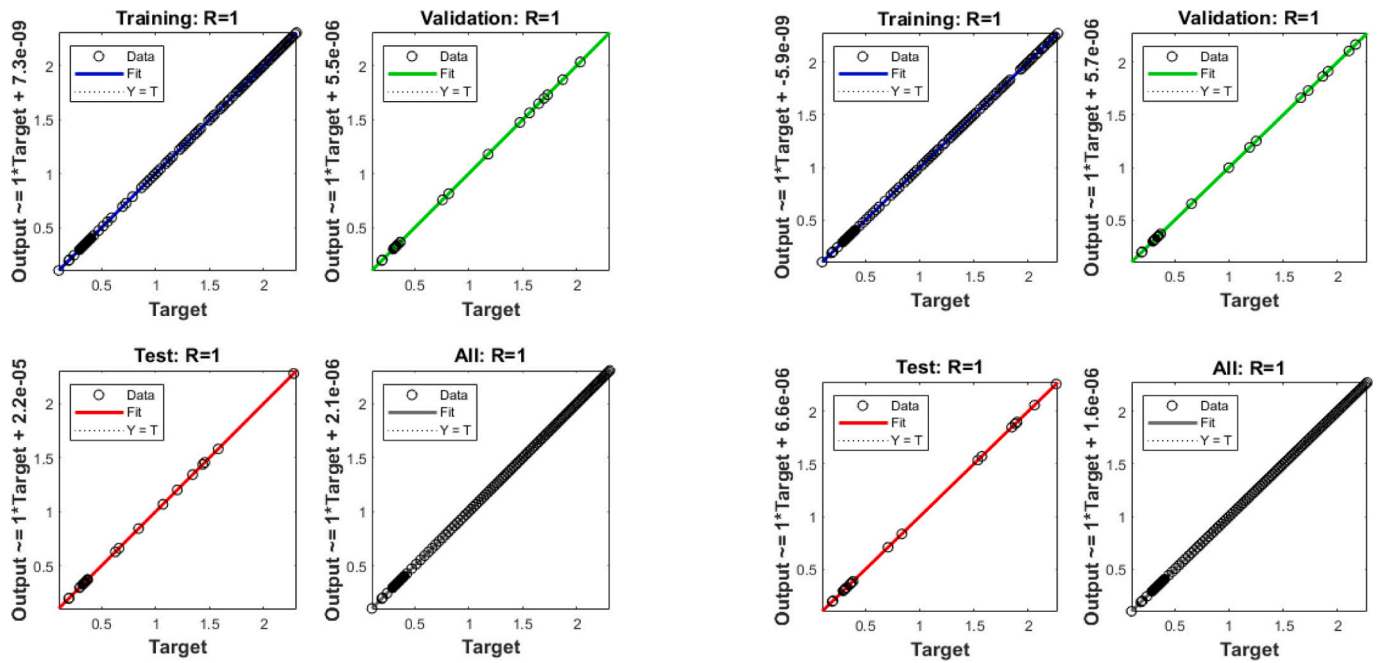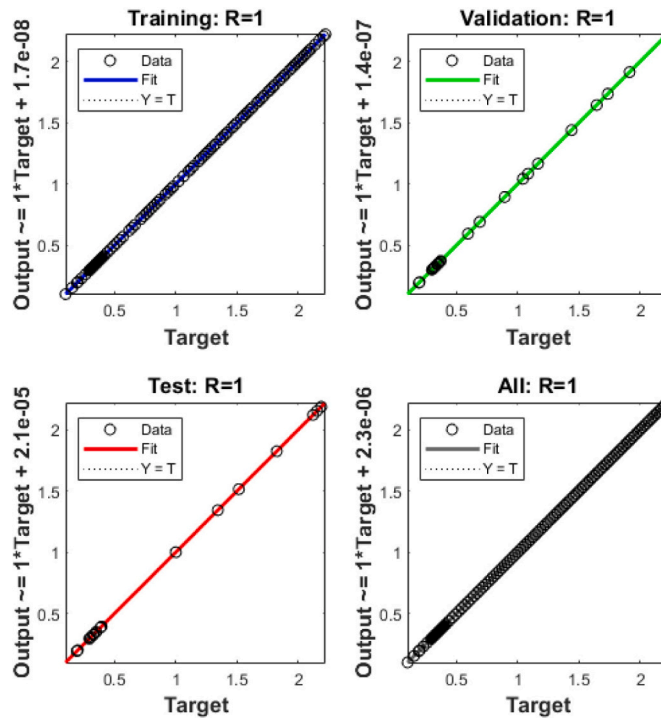Chaos, Solitons and Fractals: the interdisciplinary journal of Nonlinear Science, and Nonequilibrium and Complex Phenomena 180 (2024) 114562

Fig. 4. MSE and EHs values to solve the nonlinear FO-KFM, (a) Fit Func (1), (b) Fit Function (2), (c) Fit Func (3).

Z. Sabir et al.

Chaos, Solitons and Fractals: the interdisciplinary journal of Nonlinear Science, and Nonequilibrium and Complex Phenomena 180 (2024) 114562

(a) Reg values (1)

(b) Reg values (2)

(c) Reg values (3)

Fig. 5. Performances of Reg for the mathematical FO-KFM, (a) Reg values (1), (b) Reg values (2), (c) Reg values (3).

shown as 6.41316×10^{-10}, 5.57853×10^{-10} and 4.36235×10^{-11} at epochs 610, 868 and 286. The values of the gradient are shown in Fig. 3, which are calculated as 9.9804×10^{-08}, 9.9974×10^{-08} and 9.9629×10^{-08}. The fitting curve illustrations are presented in Fig. 4 to get the numerical results of FO-KFM, which shows the exactness of the SCJGNNs. The performances of EHs using the testing, training and

corroboration are presented in Fig. 4 calculated as -6.10×10^{-07}, 5.80×10^{-06} and 1.45×10^{-05}. The regression (Reg) illustrations are provided in Fig. 5, which have been performed as 1 for each case of mathematical FO-KFM, which shows the accuracy of proposed scheme for the FO-KFM. MSE performances for each case of the FO-KFM are shown in Table 2.

Table 2

Statistics illustrations to solve the nonlinear FO-KFM.

Case	MSE			Iterations	Performance	Gradient	Mu	Complexity
	Train	Test	Endorsement					
1	1.1512×10^{-09}	2.2568×10^{-11}	6.4131×10^{-10}	610	1.15×10^{-09}	9.98×10^{-08}	1×10^{-09}	03 Sec
2	2.2559×10^{-11}	1.5239×10^{-09}	5.5785×10^{-10}	868	2.26×10^{-11}	1.00×10^{-07}	1×10^{-10}	03 Sec
3	4.0211×10^{-11}	6.2303×10^{-09}	4.3623×10^{-11}	286	4.02×10^{-11}	9.96×10^{-08}	1×10^{-10}	01 Sec

(a) Results: Susceptible (b) Results: Infected (c) Results: Recovered (d) Results: Water components
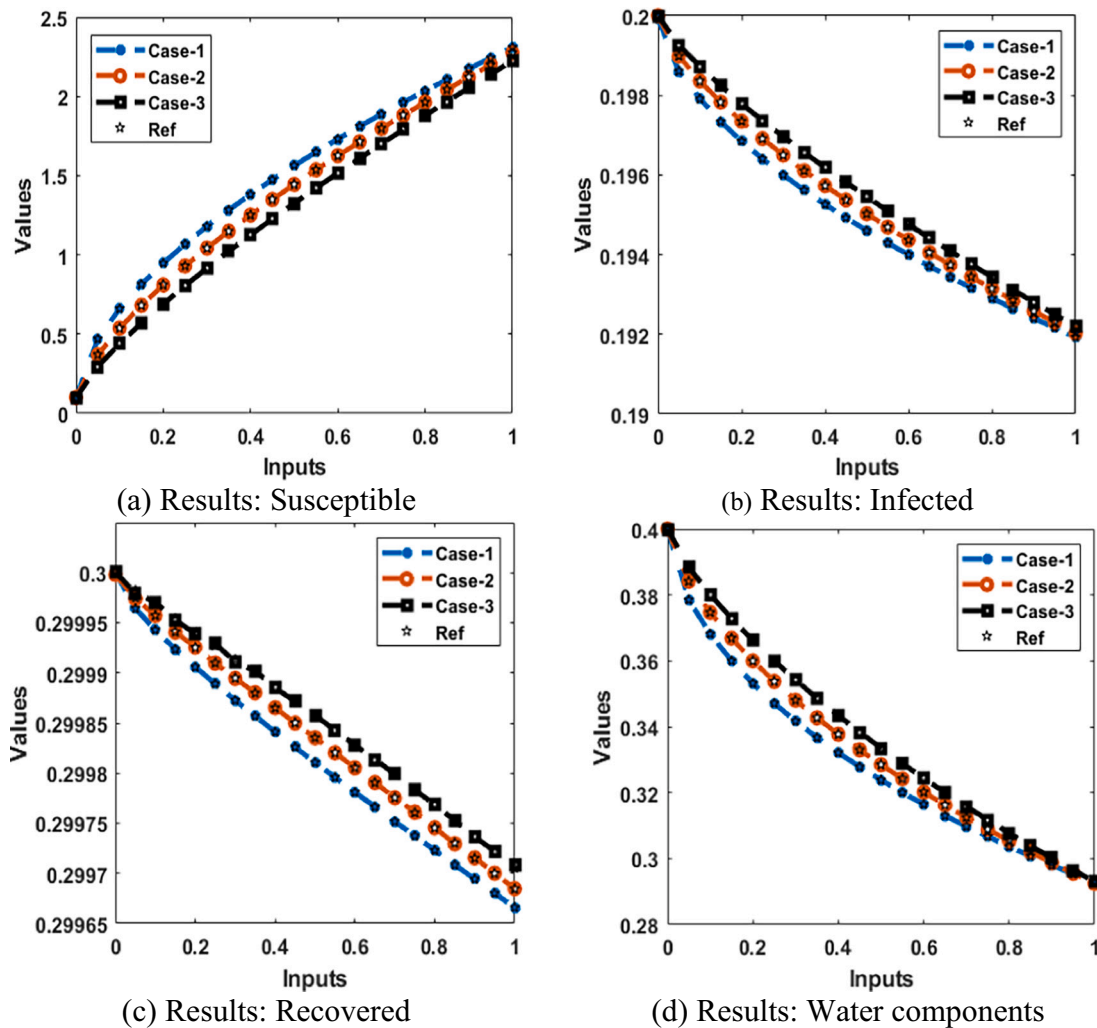
Fig. 6. Solution performances for each class of the FO-KFM, (a) Results: Susceptible, (b) Results: Infected, (c) Results: Recovered, (d) Results: Water components.

Figs. 6 and 7 present the comparison performances and AE for the FO-KFM using the designed SCJGNNs procedure. Fig. 6 shows the output comparison, which is performed through the results matching. The results matching provide the exactness and accuracy of FO-KFM. Fig. 7 depicts the AE measures for FO-KFM through the designed SCJGNNs that is divided into human and water components. The values of AE for first class (susceptible) are shown for case 1 to 3 as 10^{-04}–10^{-05}, 10^{-05}–10^{-07} and 10^{-04}–10^{-06}. For the 2nd category (infected), the AE measures are reported as 10^{-05}–10^{-08}, 10^{-06}–10^{-09} and 10^{-06}–10^{-10} for case 1 to 3. The third class (recovered) values are shown as 10^{-05}–10^{-07}, 10^{-06}–10^{-08} and 10^{-05}–10^{-08} for case 1 to 3, whereas the performances of AE water components are noticed as 10^{-05}–10^{-08}, 10^{-06}–10^{-08} and 10^{-06}–10^{-07} for respective cases. These reduceable performances of AE depict the consistency of the procedure to solve the FO-KFM.

5. Concluding remarks

The numerical performances of the fractional order kidney function model have been reported in this study. The nonlinear KFM has been separated into human (infected, susceptible, recovered) and the water components (calcium, magnesium). Few concluding comments of this study are presented as:

- The fractional derivatives in this work have been used to find the accurate results of mathematical FO-KFM.
- Three FO-KFM cases have been solved by applying the stochastic computing SCJGNNs performances.
- The statics selection is performed to solve the FO-KFM, which is used as 78 % for authorization, and 11 % for both testing and training.
- The exactness of stochastic SCJGNNs has been provided by applying the obtained and reference solutions.
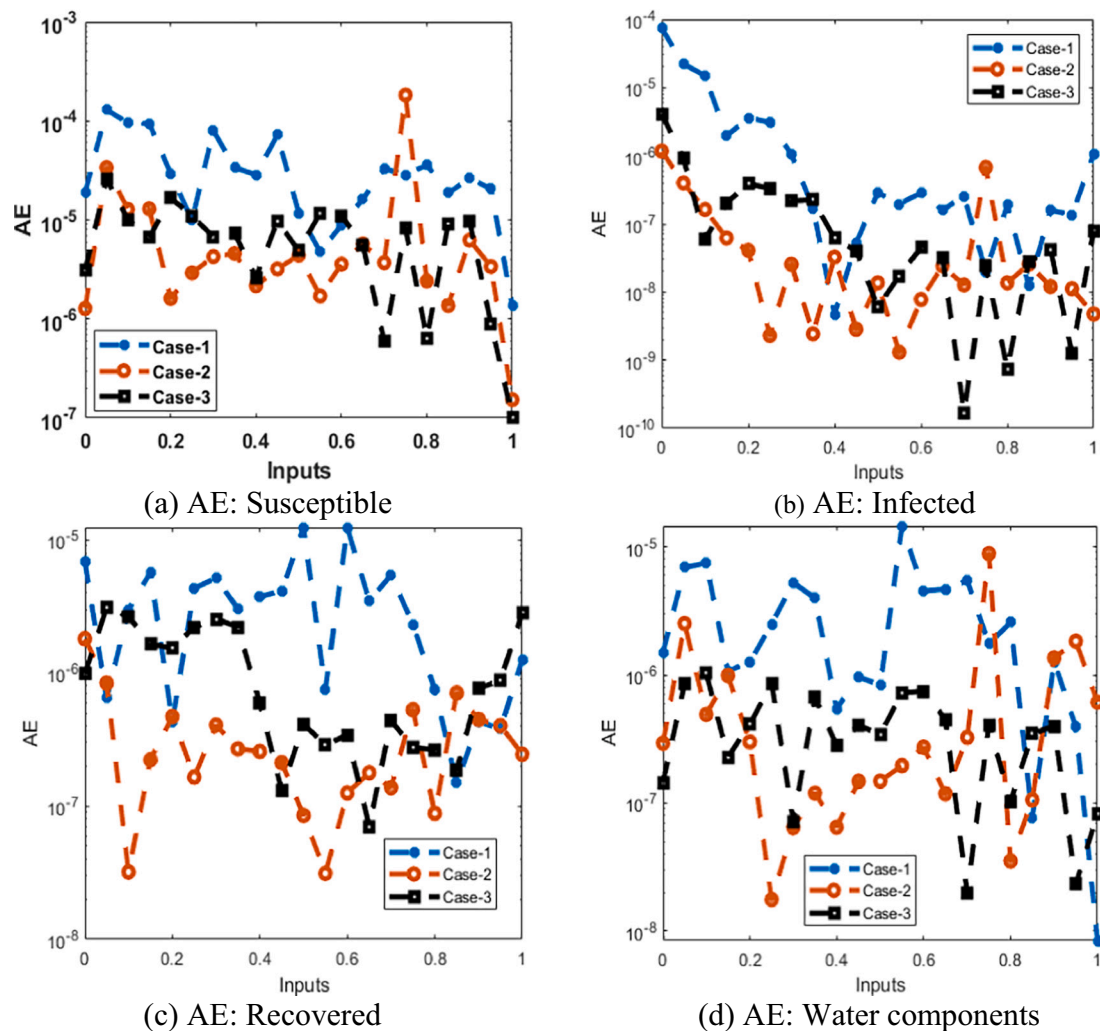
(a) AE: Susceptible

(b) AE: Infected

(c) AE: Recovered

(d) AE: Water components

Fig. 7. Values of AE for each category of the mathematical FO-KFM, (a) AE: Susceptible, (b) AE: Infected, (c) AE: Recovered, (d) AE: Water components.

- The performances of the reference solutions have been achieved by applying the Adam scheme.
- The competence and rationality have been observed through the stochastic SCJGNNs, while the simulations through the state transition, regression performances, correlation, and error histograms measures.

In upcoming studies, the process of DNNs with different schemes can be executed to perform the solutions of the fractional, fluid, and different biology based differential systems [17,18,19,20].

CRediT authorship contribution statement

Zulqurnain Sabir: Conceptualization, Methodology, Writing – original draft, Writing – review & editing. **Shahid Ahmad Bhat:** Conceptualization, Methodology, Validation, Writing – review & editing. **Hafiz Abdul Wahab:** Supervision, Writing – review & editing. **Maria Emilia Camargo:** Supervision, Validation. **Gulmira Abildinova:** Supervision, Visualization. **Zhandos Zulpykhar:** Formal analysis, Supervision.

Declaration of competing interest

All the authors of the manuscript declare that there are no potential conflicts of interest.

Data availability

No data was used for the research described in the article.

References

[1] Yang CY, Cheng MF, Tsai SS, Hsieh YL. Calcium, magnesium, and nitrate in drinking water and gastric cancer mortality. Jpn J Cancer Res 1998;89(2):124–30.
[2] Hemmelgarn BR, et al. Progression of kidney dysfunction in the community-dwelling elderly. Kidney Int 2006;69(12):2155–61.
[3] Jeraman F, et al. Sistem Pakar Diagnosa Penyakit pada Tanaman Padi Kecamatan Satarmese Kabupaten Manggarai Provinsi Nusa Tenggara Timur Berbasis Web dengan Metode Forward Chaining. Comput J 2023;1(1):73–81.
[4] Burns JA, et al. Feed-forward neural networks in chemistry: mathematical systems for classification and pattern recognition. Chem Rev 1993;93(8):2583–601.
[5] Verma P, et al. Review of mathematical modeling on latent heat thermal energy storage systems using phase-change material. Renew Sustain Energy Rev 2008;12 (4):999–1031.
[6] Razmjooy N, et al. A real-time mathematical computer method for potato inspection using machine vision. Comput Math Appl 2012;63(1):268–79.
[7] Ruttanaprommarin N, et al. Artificial neural network procedures for the waterborne spread and control of diseases. AIMS Math 2023;8(1):2435–52.
[8] de Pillis LG, et al. A validated mathematical model of cell-mediated immune response to tumor growth. Cancer Res 2005;65(17):7950–8.
[9] Wahab HA, et al. Heterogeneous/homogeneous and inclined magnetic aspect of infinite shear rate viscosity model of Carreau fluid with nanoscale heat transport. Arab J Chem 2023;16(5):104682.
[10] Yan L, et al. Design of a computational heuristic to solve the nonlinear Liénard differential model. Comput Model Eng Sci 2023;136:201–21.
[11] Sabir Z. Stochastic numerical investigations for nonlinear three-species food chain system. Int J Biomath 2022;15(04):2250005.

[12] Tambaru D, et al. The effects of hard water consumption on kidney function: insights from mathematical modelling. In: AIP conference proceedings. vol. No. 1. AIP Publishing LLC; 1937. p. 020020.

[13] Pratap A, et al. Further results on asymptotic and finite-time stability analysis of fractional-order time-delayed genetic regulatory networks. Neurocomputing 2022; 475:26–37.

[14] Zhang Z, Zou J, Upadhyay RK, Pratap A. Stability and Hopf bifurcation analysis of a delayed tobacco smoking model containing snuffing class. Adv Differ Equ 2020; 2020(1):1–19.

[15] Anbalagan P, Hincal E, Ramachandran R, Baleanu D, Cao J, Niezabitowski M. A Razumikhin approach to stability and synchronization criteria for fractional order time delayed gene regulatory networks. 2021.

[16] Nambiar, V.B., Ramamurthy, B. and Veeresha, P., Gender determination from periocular images using deep learning based EfficientNet architecture. Int J Math Comput Eng.

[17] Erdogan F. A second order numerical method for singularly perturbed Volterra integro-differential equations with delay. Int J Math Comput Eng 2024;2(1):85–96.

[18] Javeed, S. and Hincal, E., Solving coupled non-linear higher order BVPs using improved shooting method. Int J Math Comput Eng.

[19] Shoaib M, et al. A stochastic numerical analysis based on hybrid NAR-RBFs networks nonlinear SITR model for novel COVID-19 dynamics. Comput Methods Programs Biomed 2021;202:105973.

[20] Shoaib M, et al. Neuro-computing networks for entropy generation under the influence of MHD and thermal radiation. Surf Interfaces 2021;25:101243.